

# Journal of Biomedical Optics

[SPIEDigitalLibrary.org/jbo](http://SPIEDigitalLibrary.org/jbo)

## ***In vivo* imaging of human adipose-derived stem cells in Alzheimer's disease animal model**

Sungji Ha  
Sangzin Ahn  
Saeromi Kim  
Yuyoung Joo  
Young Hae Chong  
Yoo-Hun Suh  
Keun-A Chang

# *In vivo* imaging of human adipose-derived stem cells in Alzheimer's disease animal model

Sungji Ha,<sup>a</sup> Sangzin Ahn,<sup>b</sup> Saeromi Kim,<sup>b</sup> Yuyoung Joo,<sup>a</sup> Young Hae Chong,<sup>c</sup> Yoo-Hun Suh,<sup>b,d</sup> and Keun-A Chang<sup>a</sup>

<sup>a</sup>Gachon University of Medicine and Science, Department of Pharmacology, Incheon, Republic of Korea

<sup>b</sup>Seoul National University, College of Medicine, Department of Pharmacology, Seoul, Republic of Korea

<sup>c</sup>Ewha Womans University, Ewha Medical Research Institute, School of Medicine, Department of Microbiology, Seoul, Republic of Korea

<sup>d</sup>Korea Brain Research Institute (KBRI), Daegu, Republic of Korea

**Abstract.** Stem cell therapy is a promising tool for the treatment of diverse conditions, including neurodegenerative diseases such as Alzheimer's disease (AD). To understand transplanted stem cell biology, *in vivo* imaging is necessary. Nanomaterial has great potential for *in vivo* imaging and several noninvasive methods are used, such as magnetic resonance imaging, positron emission tomography, fluorescence imaging (FI) and near-infrared FI. However, each method has limitations for *in vivo* imaging. To overcome these limitations, multimodal nanoprobe have been developed. In the present study, we intravenously injected human adipose-derived stem cells (hASCs) that were labeled with a multimodal nanoparticle, LEO-LIVE™-Magnoxide 675 or 797 (BITERIALS, Seoul, Korea), into Tg2576 mice, an AD mouse model. After sequential *in vivo* tracking using Maestro Imaging System, we found fluorescence signals up to 10 days after injection. We also found strong signals in the brains extracted from hASC-transplanted Tg2576 mice up to 12 days after injection. With these results, we suggest that *in vivo* imaging with this multimodal nanoparticle may provide a useful tool for stem cell tracking and understanding stem cell biology in other neurodegenerative diseases. © The Authors. Published by SPIE under a Creative Commons Attribution 3.0 Unported License. Distribution or reproduction of this work in whole or in part requires full attribution of the original publication, including its DOI. [DOI: 10.1117/1.JBO.19.5.051206]

Keywords: *In vivo* imaging; nanoparticle; fluorescence imaging; human adipose-derived stem cells; Alzheimer's disease.

Paper 130553SPR received Aug. 1, 2013; revised manuscript received Oct. 22, 2013; accepted for publication Oct. 28, 2013; published online Dec. 2, 2013.

## 1 Introduction

Stem cell therapy has been proposed as a treatment for brain damage, spinal cord injuries, cancer, cardiovascular disease, and other conditions.<sup>1-4</sup> In fact, intravenous (i.v.) stem cell delivery for treatment has been increasingly used in animal models and humans.<sup>5,6</sup> One challenge associated with the therapeutic effects of stem cells is the lack of reliable *in vivo* imaging methods to evaluate the biology of transplanted stem cells.<sup>7</sup> An appropriate *in vivo* live imaging method is important to understand basic stem cell biology, including cell survival, migration, and differentiation after transplantation.<sup>1</sup>

Recently, nanotechnologies have contributed to advances in high resolution *in vivo* imaging for stem cell tracking.<sup>8-10</sup> Magnetic nanoparticle- or radionuclide-labeled stem cells can be visualized by magnetic resonance imaging (MRI) or by positron emission tomography (PET). MRI imaging provides high spatial resolution and anatomical information but has limited sensitivity.<sup>11,12</sup> PET imaging has high sensitivity but low spatial resolution, does not provide anatomical data, and the radioisotopes have a short half-life.<sup>8,12</sup> Fluorescence imaging (FI) with nanoparticles is another noninvasive imaging method for *in vivo* tracking. FI has advantages in high sensitivity and resolution at the subcellular level with microscopy, but has a limited penetration depth through tissues.<sup>12</sup> Near-infrared fluorescence imaging (NIRFI) has improved penetration depth and provides more specific signals, but has the limitation of photobleaching.<sup>12,13</sup> To

overcome the limitations of each single method, multimodal imaging methods have been developed.<sup>14-16</sup>

In the present study, we monitored the human adipose-derived stem cells (hASCs) in Tg2576, an Alzheimer's disease (AD) mouse model, using a multimodal MRI nanoparticle with enhanced NIR fluorescence.<sup>12</sup> hASCs were labeled with fluorescent magnetic nanoparticles (LEO-LIVE™-Magnoxide 675 or 797) and administered by tail-vein injection. Since blood-brain barrier (BBB) leakage in AD brains has been reported,<sup>17,18</sup> it was expected that intravenously injected hASCs could pass through the BBB. We checked the cellular internalization of nanoparticles into hASCs *in vitro* and performed sequential *in vivo* imaging at 0, 1, 3, and 10 days after injection using Maestro Imaging System. As a result, we could follow fluorescence signals up to 10 days after injection in live animals and found strong signals in the brains extracted from hASC-transplanted Tg2576 mice up to 12 days after injection.

## 2 Methodology

### 2.1 Cell Preparation

hASCs were prepared under GMP conditions in the Stem Cell Research Center of RNL BIO (Seoul, Korea), with approval from the Institutional Review Board of ASAN Medical Center. All hASCs were isolated from human adipose tissues obtained from disposed lower abdomen by agreement and primarily cultured as previously described.<sup>19</sup> hASCs were stained with fluorescent magnetic NEO-LIVE™-Magnoxide 675 or 797 (BITERIALS, Korea) nanoparticles at 0.4 mg/ml for *in vitro* assays or i.v. injection. All procedures were performed according to the manufacturer's instructions. hASCs were incubated in

Address all correspondence to: Keun-A Chang, Gachon University, College of Medicine, Department of Pharmacology, 191 Hambakmoero, Yeonsu-Gu, Incheon 406-799, Republic of Korea. Tel: + (82)-32-820-4332; Fax: + (82)-32-820-4744; E-mail: kachang74@gmail.com

growth medium containing Magnoxide for 24 h and washed with phosphate-buffered saline (PBS).

## 2.2 Animals

All animal procedures were performed according to the National Institutes of Health Guidelines for the Humane Treatment of Animals, with approval from the Institutional Animal Care and Use Committee of Seoul National University (IACUC No. SNU-091208-1). Tg2576 mice, which express mutant human APP, Swedish (K670N/M671L) mutation, were obtained from Taconic Farms (Germantown, New York) and were bred by mating male mice with C57B16/SJL F1 females as described previously.<sup>20</sup> Mouse genotyping was performed as recommended by Taconic Farms. Eleven-month-old male Tg2576 mice or age-matched WT mice were injected with  $150 \mu\text{l}$  of  $1 \times 10^6$  hASCs suspension through the tail vein.

## 2.3 Immunocytochemistry

hASCs labeled with Magnoxide 675 were fixed with 4% paraformaldehyde in PBS for 10 min at room temperature (RT), permeabilized with 0.2% Triton X-100 in PBS for 5 min, and blocked with 5.0% normal goat serum (Vector Laboratories, California) in PBS for 1 h at RT. They were then incubated with anti-human nuclei antibody (1:100, Millipore, Massachusetts) for 1 h at RT, washed with PBS three times and incubated with secondary antibody, Alexa Fluor® 488 Anti-Mouse IgG (1:500, Invitrogen, California) and 4',6-diamidino-2-phenylindole (DAPI) for 1 h at RT. After washing with PBS three times, the coverslips were mounted and observed under a Zeiss LSM 510 confocal imaging system (Zeiss, Heidelberg, Germany).

## 2.4 *In vivo* fluorescence imaging

Fluorescence images were obtained using a Maestro Imaging System (CRI Inc., Woburn, Massachusetts) for data acquisition and analysis. For effective detection, fur on the dorsal and ventral sides of the mice was removed 1 day prior to imaging. The mice were anesthetized and  $1 \times 10^6$  hASCs labeled with NEO-LIVE™-Magnoxide 675 or 797 were injected through the tail-vein. The first *in vivo* images were captured at 5 min after the injections. With the mice under anesthesia, sequential *in vivo*

fluorescence measurements were taken at 1, 3, and 10 days post-injection using the Maestro equipment. To examine the distribution of the transplanted cells, all organs were extracted at 5 or 12 days after injection and images were captured.

## 3 Results and Discussion

The effective cellular internalization of nanoparticles into hASCs was observed by confocal microscopy as shown in Fig. 1. Cells were incubated with Magnoxide 675 in culture medium for 24 h and stained with anti-human nuclei antibody to detect nuclei of human cells. Magnoxide 675 was internalized into the cells and mainly resided in the cytoplasm. In the previous report, Park et al.<sup>21</sup> showed that internalized nanoparticles are stable in the cells and are cytocompatible. We also confirmed that there were no cytotoxicity and no change on the overall growth rate or morphology of hASCs (Fig. 1).

For *in vivo* cell tracking, cells were labeled with Magnoxide 797 1 day before injection. Labeling of cells was confirmed using Maestro Image System before the tail-vein injection [Fig. 2(a)]. *In vivo* fluorescence images were captured according to the experimental scheme in Fig. 2(b). The first images, which were obtained 5 min after injection, showed almost no fluorescence signal [Fig. 2(c), left panel]. One day after injection, hASCs were detected in the tail, body, and brain especially in the Tg2576 mouse (Tg-hASC). Since the AD brain shows leakage of the BBB, it is likely that hASCs could pass through the BBB and could be detected in the brain. Otherwise, no signal was observed in WT-hASC mice brain [Fig. 2(c), second panel]. At 3 days after injection, the fluorescence signals from hASCs in the brains were higher than those on any other days. To exclude autofluorescence signals, we took images of Tg-hASC mice together with WT-Sham (injected with saline) mice in the same field. Although the fluorescence signals decayed as time passed, we found weak signals at 10 days after injection. No signal was observed at 17 and 30 days after injection (data not shown).

To examine the organ distribution of the transplanted cells, organs were extracted at 5 or 12 days after injection and then visualized using Maestro Image System. These mice were injected with saline or stem cells labeled with NEO-LIVE™-Magnoxide 675. Compared with WT-Sham or WT-hASC mice, Tg2576 mice showed high fluorescence signals in all organs including brain, gastrointestinal (GI) tract, kidney,

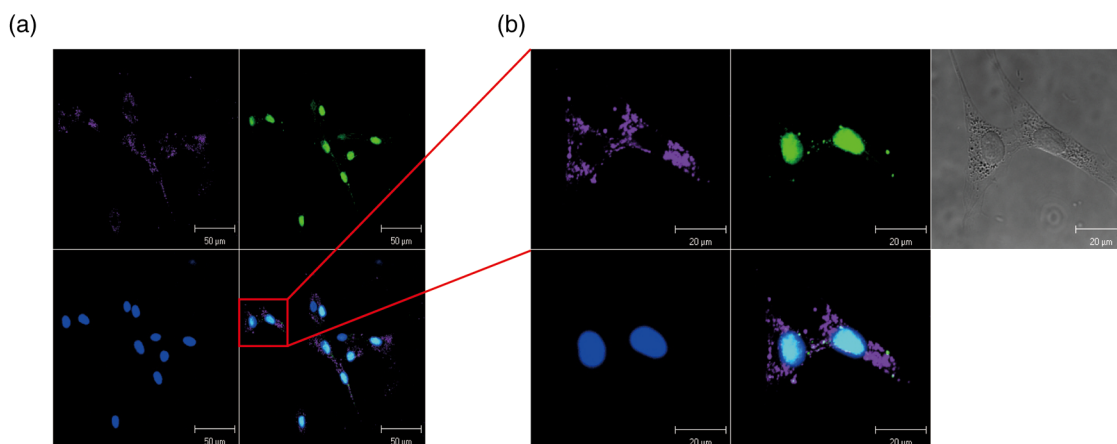


**Fig. 1** (a) Confocal microscope images of human adipose-derived stem cells (hASCs) labeled with NEO-LIVE™-Magnoxide 675 (purple). Cells were stained with anti-human nuclei (green) and DAPI (blue). Scale bar,  $50 \mu\text{m}$  (b) Magnified images of the red squares in the left panels. Scale bar,  $20 \mu\text{m}$ .

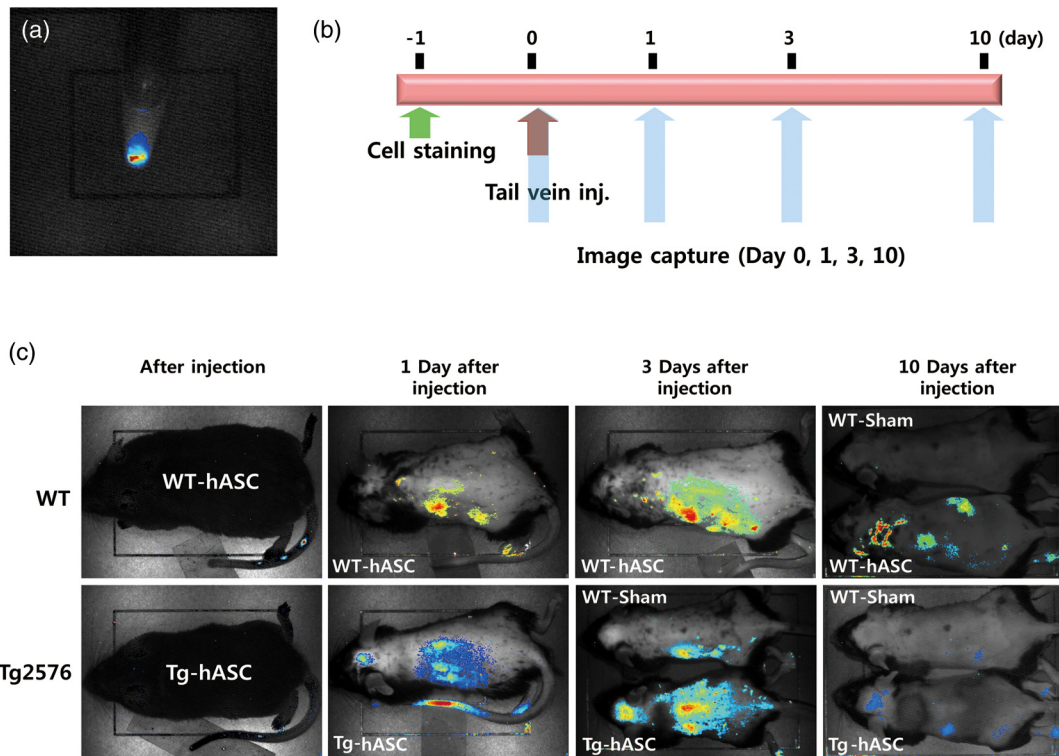


**Fig. 2** (a) Labeled cells with NEO-LIVE™-Magnoxide 797 in EP tube were visualized using Maestro Imaging System. (b) Experimental scheme of image measurements. (c) Sequential *in vivo* tracking was performed in mice injected with NEO-LIVE™-Magnoxide 797-labeled hASCs. Fluorescent images were taken at the indicated times. WT/hASC: injected with nanolabeled hASCs, WT-Sham: injected with saline.

liver, and bladder. Because the GI tract showed too strong signal to analyze other organs, we excluded it from the result [Fig. 3(a)]. Tg-hASC-2, which was sacrificed at 5 days after injection, showed much higher signals than Tg-hASC-1, sacrificed at 12 days after injection [Fig. 3(a)]. Additionally, we compared all signals from the brains in the same field and found strong signals in the Tg-hASC mice brains [Fig. 3(b)].

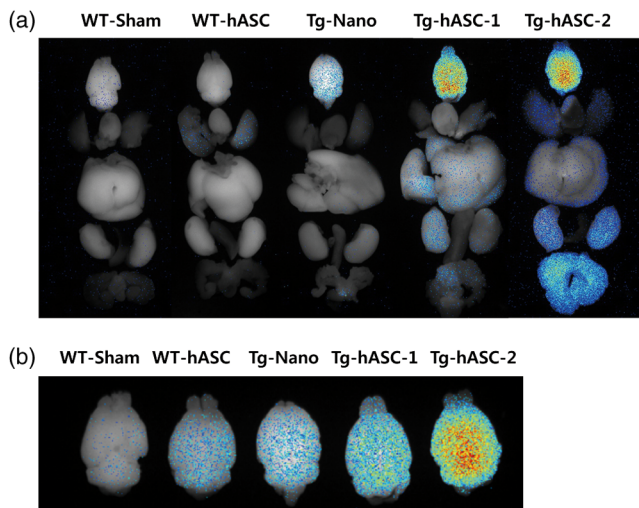


**Fig. 3** (a) Mice were injected with saline, NEO-LIVE™-Magnoxide 675-labeled hASCs or nanoparticle only. Each organ was extracted at 5 or 12 days after injection (only Tg-hASC-2 was sacrificed at 5 days after injection) and images were captured using Maestro Imaging System. (b) Brain images were captured separately in the same field. WT-Sham: injected with saline, Tg-Nano: injected with nanoparticles, and WT/hASC: injected with nanolabeled hASCs.

There were weak signals in the brains in the WT-ASC or Tg-Nano mice brain. According to recent report which showed transmigration of the mesenchymal stem cells across the BBB,<sup>22</sup> it is likely that some cells are able to enter the WT mice brains. However, labeled hASCs were shown much more in the brains of Tg mice than in those of WT mice (Fig. 3). Stability of internalized nanoparticles has been previously confirmed, so it might be inferred that fluorescent signals in the brains came from hASC.<sup>21</sup>

Since NEO-LIVE™-Magnoxide 675 is a multimodal nanoparticle which is suitable for optical imaging and MRI, MRI was performed to examine further anatomical information of transplanted cells in the brain. The result indicated that some signals from hASCs labeled with nanoparticles were detected at 2 and 7 days after transplantation in the cortex area (data not shown). For more defined information, additional confirmation is required.

In summary, for *in vivo* imaging of stem cells in AD mouse model, we intravenously administered stem cells labeled with fluorescent magnetic nanoparticles through the tail-vein. We successfully follow the fluorescent signals from hASCs in AD mouse model until 10 days after injection. Up to 12 days after injection, strong signals were found in the brains extracted from hASC-transplanted Tg2576 mice. These results suggest that *in vivo* imaging with this multimodal nanoparticle may provide a useful tool for stem cell tracking and understanding stem cell biology in other neurodegenerative diseases.

#### Acknowledgments

This work was supported by the Gachon University research fund of 2012 (GCU-2012-M084).



## References

1. S. C. Li et al., "A biological global positioning system: considerations for tracking stem cell behaviors in the whole body," *Stem Cell Rev.* **6**(2), 317–333 (2010).
2. M. I. Phillips, Y. L. Tang, and K. Pinkernell, "Stem cell therapy for heart failure: the science and current progress," *Future Cardiol.* **4**(3), 285–298 (2008).
3. N. Sandu and B. Schaller, "Stem cell transplantation in brain tumors: a new field for molecular imaging?," *Mol. Med.* **16**(9–10), 433–437 (2010).
4. A. C. Lepore and N. J. Maragakis, "Stem cell transplantation for spinal cord neurodegeneration," *Methods Mol. Biol.* **793**, 479–493 (2011).
5. U. M. Fischer et al., "Pulmonary passage is a major obstacle for intravenous stem cell delivery: the pulmonary first-pass effect," *Stem Cells Dev.* **18**(5), 683–691 (2009).
6. U. Krause et al., "Intravenous delivery of autologous mesenchymal stem cells limits infarct size and improves left ventricular function in the infarcted porcine heart," *Stem Cells Dev.* **16**(1), 31–37 (2007).
7. J. Chung and P. C. Yang, "Molecular imaging of stem cell transplantation in myocardial disease," *Curr. Cardiovasc. Imaging Rep.* **3**(2), 106–112 (2010).
8. C. Villa et al., "Stem cell tracking by nanotechnologies," *Int. J. Mol. Sci.* **11**(3), 1070–1081 (2010).
9. L. Ferreira et al., "New opportunities: the use of nanotechnologies to manipulate and track stem cells," *Cell Stem Cell* **3**(2), 136–146 (2008).
10. R. Singh and H.S. Nalwa, "Medical applications of nanoparticles in biological imaging, cell labeling, antimicrobial agents, and anticancer nanodrugs," *J. Biomed. Nanotechnol.* **7**(4), 489–503 (2011).
11. V. S. Lelyveld et al., "Challenges for molecular neuroimaging with MRI," *Int. J. Imaging Syst. Technol.* **20**(1), 71–79 (2010).
12. J. S. Kim et al., "Development and in vivo imaging of a PET/MRI nanoprobe with enhanced NIR fluorescence by dye encapsulation," *Nanomedicine* **7**(2), 219–229 (2012).
13. S. Nagarajan and Y. Zhang, "Upconversion fluorescent nanoparticles as a potential tool for in-depth imaging," *Nanotechnology* **22**(39), 395101 (2011).
14. C. K. Sung et al., "Dual-modal nanoprobe for imaging of mesenchymal stem cell transplant by MRI and fluorescence imaging," *Korean J. Radiol.* **10**(6), 613–622 (2009).
15. A. Tennstaedt et al., "Noninvasive multimodal imaging of stem cell transplants in the brain using bioluminescence imaging and magnetic resonance imaging," *Methods Mol. Biol.* **1052**, 1–14 (2013).
16. L. Stelter et al., "Modification of aminosilanized superparamagnetic nanoparticles: feasibility of multimodal detection using 3T MRI, small animal PET, and fluorescence imaging," *Mol. Imaging Biol.* **12**(1), 25–34 (2010).
17. G. L. Bowman et al., "Blood-brain barrier impairment in Alzheimer disease: stability and functional significance," *Neurology* **68**(21), 1809–1814 (2007).
18. B. D. Zipser et al., "Microvascular injury and blood-brain barrier leakage in Alzheimer's disease," *Neurobiol. Aging* **28**(7), 977–986 (2007).
19. J. C. Ra et al., "Safety of intravenous infusion of human adipose tissue-derived mesenchymal stem cells in animals and humans," *Stem Cells Dev.* **20**(8), 1297–1308 (2011).
20. K. Hsiao et al., "Correlative memory deficits, Abeta elevation, and amyloid plaques in transgenic mice," *Science* **274**(5284), 99–102 (1996).
21. K. S. Park et al., "Characterization, in vitro cytotoxicity assessment, and in vivo visualization of multimodal, RITC-labeled, silica-coated magnetic nanoparticles for labeling human cord blood-derived mesenchymal stem cells," *Nanomed. Nanotechnol. Biol. Med.* **6**(2), 263–276 (2010).
22. M. N. Lin et al., "Involvement of PI3K and ROCK signaling pathways in migration of bone marrow-derived mesenchymal stem cells through human brain microvascular endothelial cell monolayers," *Brain Res.* **1513**, 1–8 (2013).